Am J Nucl Med Mol Imaging 2014;4(6):561-570
www.ajnmmi.us /ISSN:2160-8407/ajnmmi0001271

Original Article

In vivo phage display selection of an ovarian cancer targeting peptide for SPECT/CT imaging

Mette Soendergaard[1], Jessica R Newton-Northup[1], Susan L Deutscher[1,2]

[1]Department of Biochemistry, University of Missouri, Rm117 Schweitzer Hall, Columbia, MO 65211; [2]Harry S. Truman Memorial Veterans Hospital, 1 Hospital Drive, Columbia, MO 65201

Received July 1, 2014; Accepted July 17, 2014; Epub September 6, 2014; Published September 15, 2014

Abstract: The often fatal outcome of ovarian cancer (OC) is related to inadequate detection methods, which may be overcome by development of nuclear imaging agents. Cancer targeting peptides have been identified using *in vivo* bacteriophage (phage) display technology; however, the majority of these ligands target tumor vasculature. To overcome this problem, a two-tier phage display method was employed to select an ovarian cancer targeting peptide with good pharmacokinetic and imaging properties. A fUSE5 15-amino acid peptide library was screened against xenografted human OC SKOV-3 tumors in mice, which was followed by selection against enriched SKOV-3 cells. The selected peptide RSLWSDFYASASRGP (J18) was synthesized with a GSG-spacer and a 1,4,7,10-tetraazacyclodecane-1,4,7,10-tetraacetic acid (DOTA) chelator and radiolabeled with ^{111}In. SKOV-3 xenografted mice were used to evaluate the biodistribution and single photon emission computed tomography (SPECT) imaging capabilities of the radiolabeled peptide. Competitive binding experiments using ^{111}In-DOTA-GSG-J18 indicated that the peptide displayed a half maximal inhibitory concentration (IC_{50}) value of 10.5 ± 1.1 μM. Biodistribution studies revealed that tumor uptake was 1.63 ± 0.68, 0.60 ± 0.32, 0.31 ± 0.12 and 0.10 ± 0.02% injected dose/g at 30 min, 1 h, 2 h and 4 h post-injection of ^{111}In-DOTA-GSG-J18, respectively. SPECT/CT imaging demonstrated good tumor uptake and minimal background binding. This study demonstrated successful utilization of a two-tier phage display selection process to identify an ovarian cancer avid peptide with excellent SPECT/CT imaging capabilities.

Keywords: Ovarian cancer, peptide, phage display, SPECT imaging

Introduction

Ovarian cancer (OC) is the fifth leading cause of cancer deaths in women, and has been termed the silent killer due to a predominantly asymptomatic disease development and quick dissemination of aggressive metastatic cells. The late manifestations of OC cause ~70% of patients to be diagnosed at advanced stage disease, at which point five-year survival rates are merely 30-45%. In contrast, the minority of women diagnosed at the early stages of OC exhibit good five-year survival rates of > 90%, emphasizing the importance of diagnosis at early onset [1, 2]. Currently, standard detection methods involve evaluation of CA-125 (Mucin 16) serum levels and ultrasonography, which are both mostly successful for late-stage OC. In fact, only 50% of patients with stage I disease test positive for elevated CA-125 serum levels, which highlight the need for identification and development of efficacious detection methods of OC [3].

Various cancers have been successfully imaged using radionuclide-coupled peptides [4-6], and while these ligands generally display lower binding affinities compared to antibodies, they offer advantages in regard to tumor targeting by exhibiting low immunogenicity, rapid blood-clearance and excretion through the urine [7]. High-throughput strategies such as bacteriophage (phage) display are utilized in the discovery of such peptide ligands [8, 9]. Phage display is a well-established technique that allows selection of ligands from large phage libraries, in which random peptide sequences are displayed on coat proteins [10]. Cancer targeting peptides can be identified by *in vivo* phage display selections against tumor targets in live animals, and have resulted in peptides with great stability and biodistribution. However, most of these

Table 1. Micropanning assay to determine binding of selected phage clones to SKOV-3 and HS-832 cells

Phage No.	*Peptide sequence*	*SKOV-3 to HS-832 ratio*
pJ1	RTEVPVLSFTSPLTG	1.76
pJ2	GDVWLFKTSTSHFAR	1.91
pJ3	AREYGTRFSLIGGYR	0.21
pJ4	HAAFEPRGDVRHTLL	2.00
pJ5	LGRAGQSYPSFARGL	0.52
pJ6	PIFPVVSSSGSSSSP	1.58
pJ7	PLSHGSVVYPRSSLG	1.36
pJ8	RRDTVPRSLSAPLSW	0.59
pJ9	PAVASTSSLIIDGPF	2.29
pJ10	HPPLASVWHVSVPL	0.83
pJ11	LHDFRSPIYASLLGF	1.53
pJ12	AGDGGLGRVAAGARV	1.15
pJ13	RVFHLWPHPTSTLSA	0.25
pJ14	APLSYNFASMPFMSG	0.73
pJ15	HPGWFDSAWFRAVSR	1.24
pJ16	ARDSRCGGFLGCGVT	1.36
pJ17	AMVRGFSFGMSRGSD	1.94
pJ18	RSLWSDFYASASRGP	6.57
pJ19	SYSVVNSPWCDGTCD	1.25
pJ20	SRDGLHSFCYVGCPP	0.40
pJ21	GVGDADGFIPVISAV	0.59
pJ22	PVFFRLSPVTEGGGV	1.40
pJ23	FPSYPFIAYSLQTPV	1.23
pJ24	RRLPHLMPFEGSVFL	3.55
pJ25	GPHFDYRTGLGWRFG	1.35
pJ26	LGKGLTGSALSLSAL	2.29
pJ27	YGVTPSPRSPWATAH	3.43
pJ28	VFVDGARYSTASDSL	2.83
pJ29	GAGIFGPWGVFAAVP	1.21
pJ30	GYRSAFVPFVARGGH	3.65
pJ31	RYRVGFTPGTIAAVL	1.13

SKOV-3 or HS-832 cells were incubated with individual phage clones and eluted using 2.5% CHAPS. Phage binding was determined by titer and the SKOV-3 to HS-832 ratio was calculated.

peptides have been found to bind the tumor vasculature rather than actual cancer cells [11, 12]. Therefore, careful design of the phage display selection enables identification of peptides that are able to extravasate the vasculature, bind specific cells of interest and possess desirable pharmacokinetics.

To overcome this problem, our laboratory developed a two-tier phage display technique that involves *in vivo* selection rounds in tumor-bearing mice followed by screening against cultured tumor cells *in vitro*. In the current study, we hypothesized that this rigid selection process against xenografted human OC (SKOV-3) tumors in mice and enriched cultured SKOV-3 cells would identify peptide ligands that could be utilized in single-photon emission computed tomography (SPECT) imaging. This study resulted in identification of an OC targeting peptide RSLWSDFYASASRGP (J18), which was synthesized with a GSG-spacer and conjugated to a 1,4,7,10-tetraazacyclodecane-1,4,7,10-tetraacetic acid (DOTA)-chelator. The conjugated peptide was radiolabeled with ^{111}In and evaluated in regard to its stability and binding affinity for SKOV-3 cells. The pharmacokinetic properties and SPECT imaging capabilities of ^{111}In -DOTA-GSG-J18 were determined in SKOV-3 xenografted mice, and the results showed that the peptide exhibited good tumor targeting and retention and was able to successfully localize ovarian tumors.

Materials and methods

Chemicals and reagents

$^{111}InCl_3$ was purchased from Mallinckrodt Chemicals (St. Louis, MO). Unless otherwise stated, chemicals were obtained from Thermo Fisher Scientific (Waltham, MA).

Cell lines and cell culture

The human ovarian adenocarcinoma cell line SKOV-3 and human normal ovarian cells (HS-832) were purchased from American Type Tissue Culture. Both cell lines were cultivated in RPMI 1640 (custom) with 10% fetal bovine serum (FBS), 2 mM L-glutamine, 1.7 μM insulin and 48 mg/ml gentamicin, and maintained at 37°C in 5% CO_2.

Animals and handling

Solid tumors (1 cm) were established in 4-6-week-old female nude (nu/nu) mice (Harlan, Indianapolis, IN) over a period of 8 weeks. The animals were inoculated subcutaneously in the shoulder under gas anesthesia (3.5% isoflurane, Baxter Healthcare Corp. Deerfield, IL) with $1x10^7$ SKOV-3 cells. All animal studies were conducted according to NIH Guidelines for Care and Use of Laboratory Animals and the Policy and Procedures for Animal Research of

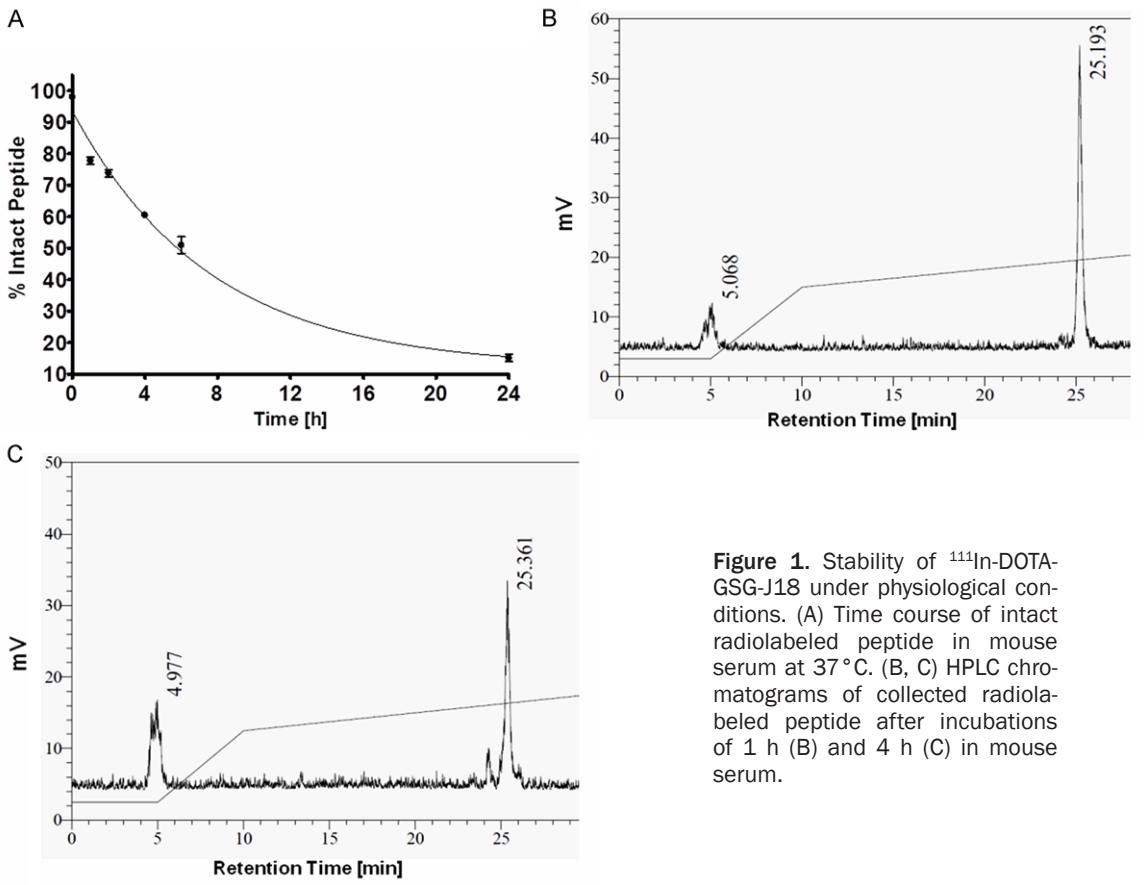

Figure 1. Stability of ^{111}In-DOTA-GSG-J18 under physiological conditions. (A) Time course of intact radiolabeled peptide in mouse serum at 37°C. (B, C) HPLC chromatograms of collected radiolabeled peptide after incubations of 1 h (B) and 4 h (C) in mouse serum.

the Harry S. Truman Veterans Memorial Hospital.

Phage display selections of tumor binding phage clones

For selection of tumor targeting phage clones, a linear 15-mer fUSE5 phage display library (a gift from Dr. George Smith) was used [10]. The library was pre-cleared from vasculature and non-tumor target binding phage according to previous methods [13]. The pre-cleared phage library (10^{12} pfu) was injected into xenografted SKOV-3 tumor-bearing nude mice and allowed to circulate for 1 h. The animals were sacrificed, tumors were collected and minced, and bound phage were eluted and amplified as previously described [13]. The selection was repeated a total of four times. Tumor-derived SKOV-3 cells were enriched using MACS® MicroBeads (Miltenyi Biotech, Auburn, CA) technology [14], and used in a final round of selection. Selected phage were analyzed for binding to SKOV-3 and HS-832 cells in a micropanning assay per previous methods [13].

Peptides

Solid-phase Fmoc chemistry was used to synthesize peptides in a 396 multiple peptide synthesizer (Advanced Chem Tech, Louisville, KY). Peptides were synthesized with a DOTA-chelator linked to a GSG-spacer at the NH_2-terminus. Purification was performed using reverse-phase high-pressure liquid chromatography (RP-HPLC; Beckmann Coulter System Gold HPLC, Beckmann Coulter, Fullerton, CA) on a C18 column (Novapack Reverse Phase, Waters, Milford, MA) and lyophilized and stored at -20°C. The peptides were identified by electrospray ionization mass spectrometry (Mass Consortium Corp, San Diego, CA).

Peptide radiolabeling and stability

The selected peptide was radiolabeled with ^{111}In (^{111}In-DOTA-GSG-J18) by incubating 100 µg peptide with 18.5 MBq ^{111}In-Cl_3 in 0.5 M NH_4-acetate buffer, pH 5.0, at 85°C for 1 h. For blocking experiments, 1 mg peptide was incubated with 10^{-4} M non-radioactive indium under

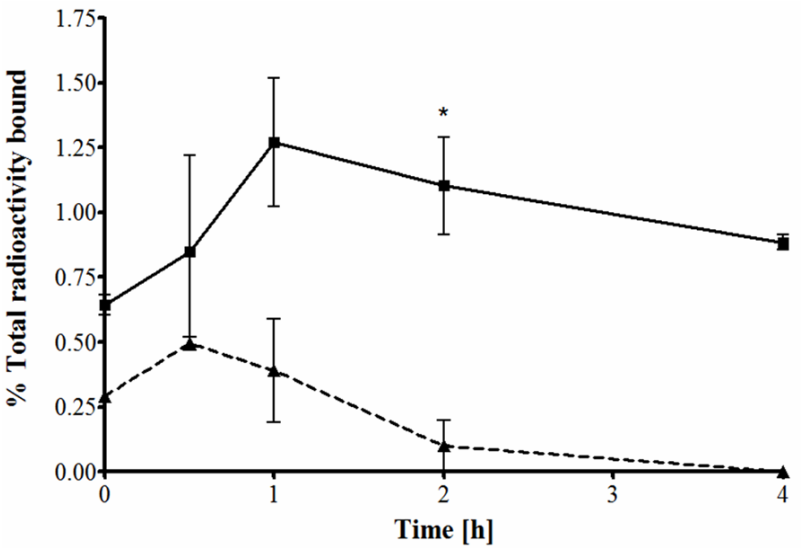

Figure 2. Binding properties of ^{111}In-DOTA-GSG-J18 to OC SKOV-3 (■) and normal ovarian HS-832 (▲) cells. Cells were incubated with radiolabeled peptide for different periods of time. Although, binding of ^{111}In-DOTA-GSG-J18 to SKOV-3 cells was significantly higher ($p < 0.05$) at 2 h, binding to HS-832 cells was also observed.

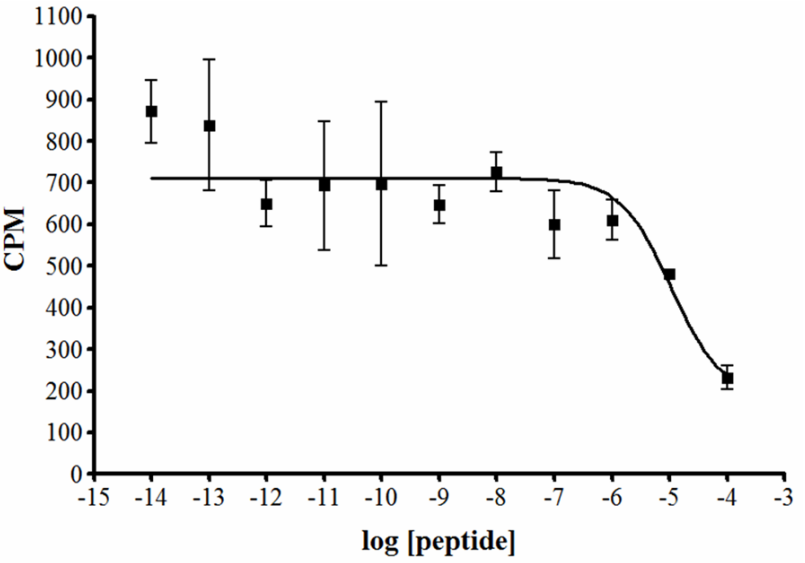

Figure 3. Cell binding competition study of ^{111}In-DOTA-GSG-J18 and its non-radioactive counterpart. SKOV-3 cells were incubated with ^{111}In-DOTA-GSG-J18 and various concentrations (10^{-14} to 10^{-4} M) of the correlating non-radiolabeled peptide In-DOTA-GSG-J18 for 1 h at 37°C. Bound radioactivity was measured and the IC_{50} value was 10.5 ± 1.1 μM (mean ± SE).

similar conditions. The non-radioactive and radiolabeled peptides were purified using RP-HPLC (LC-20A Prominence, Shimadzu, Columbia, MD) on a C18 column (Higgins Analytical Inc., Mountain View, CA; 25-35% acetonitrile/0.1% trifuoroacetic acid) over 20 min. Acetonitrile was removed by further purification on an Empore® Extraction Disk C18 cartridge (Phenomenex, Torrance, CA), and the peptide was eluted with 70% ethanol and the pH adjusted to neutral by 0.5 M 2-[4-(2-hydroxyethyl)piperazin-1-yl]ethanesulfonic acid (HEPES; final concentration) buffer. For animal experiments, the ethanol was evaporated under N_2 and the peptide was resuspended in 0.1 M HEPES buffer, pH 7. Peptide stability was analyzed in mouse serum over time (0 h, 1 h, 2 h, 4 h, 6 h and 24 h) at 37°C, and degradation was monitored by RP-HPLC on a C18 column. In short, at the end of each incubation mouse serum protein was precipitated by addition of acetonitrile, and removed by centrifugation and filtration using a 0.22 μm filter. The filtrate was then loaded onto the HPLC.

Cell binding studies

Ovarian cancer specificity of ^{111}In-DOTA-GSG-J18 was evaluated in a cell binding assay as previously described [15], except SKOV-3 or HS-832 cells ($1x10^6$) were incubated with $2x10^5$ cpm of ^{111}In-DOTA-GSG-J18 in DMEM, 1% bovine serum albumin at 37°C for different periods of time (0 min, 0.5, 1, 2 and 4 h). Bound radioactivity was measured using a Genesys™ Genii™ Multi-Well Gamma Counter (Laboratory Technologies, Inc, Maple Park, IL).

To determine the half maximal inhibitory concentration (IC_{50}) of the peptide ligand to OC

Table 2. Biodistribution of ^{111}In-DOTA-GSG-J18 in SKOV-3 tumor-bearingnude mice

Pharmacokinetics of ^{111}In-DOTA-GSG-J18					
%ID/g					
Tissues	30 min	1 h†	1 h-block	2 h‡	4 h
Tumor	1.63 ± 0.68	0.60 ± 0.32	0.31 ± 0.12*	0.18 ± 0.03	0.10 ± 0.02
Blood	2.37 ± 0.94	0.40 ± 0.24	0.23 ± 0.11	0.03 ± 0.03	0.19 ± 0.02
Heart	0.67 ± 0.27	0.13 ± 0.08	0.07 ± 0.03	0.02 ± 0.01	0.05 ± 0.01
Lung	2.42 ± 0.48	1.06 ± 0.82	0.83 ± 0.19	0.49 ± 0.36	0.62 ± 0.32
Liver	1.42 ± 0.37	0.51 ± 0.48	0.37 ± 0.02	0.23 ± 0.11	0.84 ± 0.13
Spleen	1.77 ± 0.46	0.68 ± 1.01	0.16 ± 0.03	0.19 ± 0.24	1.58 ± 0.36
Stomach	0.36 ± 0.14	0.11 ± 0.04	0.08 ± 0.03	0.04 ± 0.02	0.04 ± 0.00
Large intestine	0.34 ± 0.17	0.15 ± 0.05	0.07 ± 0.02	0.27 ± 0.06	0.28 ± 0.19
Small intestine	0.63 ± 0.29	0.32 ± 0.11	0.15 ± 0.04	0.15 ± 0.08	0.06 ± 0.01
Intestines	0.49 ± 0.22	0.25 ± 0.08	0.12 ± 0.03	0.20 ± 0.07	0.15 ± 0.08
Kidneys	6.71 ± 3.08	2.70 ± 0.95	1.98 ± 0.29	1.67 ± 0.43	1.75 ± 0.17
Brain	0.09 ± 0.03	0.03 ± 0.01	0.02 ± 0.00	0.01 ± 0.00	0.01 ± 0.00
Muscle	0.32 ± 0.17	0.06 ± 0.03	0.04 ± 0.01	0.01 ± 0.00	0.01 ± 0.00
Pancreas	0.65 ± 0.18	0.11 ± 0.05	0.08 ± 0.01	0.02 ± 0.01	0.04 ± 0.01
Bone	0.31 ± 0.13	0.06 ± 0.05	0.05 ± 0.03	0.02 ± 0.01	0.08 ± 0.02
Skin	1.28 ± 0.68	0.22 ± 0.11	0.22 ± 0.08	0.09 ± 0.03	0.10 ± 0.01
Uptake ratio					
Tumor to blood	0.69	1.50	1.35	6.00	0.53
Tumor to muscle	5.10	10.00	7.75	18.00	10.00

Data are represented as %ID/g (mean ± SD), or as uptake ratio of tumor to normal tissue for female nude mice (n=4) bearing SKOV-3 xenografted tumors. Mice were sacrificed at different times post-injection of ^{111}In-DOTA-GSG-J18. †n=7, ‡n=5, *p=0.03, significant difference between tumor uptake of radiolabeled peptide 1 h post-injection with and without the presence of its non-radioactive counterpart.

cells (SKOV-3), competition experiments were performed with the radiolabeled (^{111}In-DOTA-GSG-J18) and the non-radioactive counterpart (In-DOTA-GSG-J18) according to previous studies [15]. In brief, cells ($1x10^6$) were incubated with $2x10^5$ cpm of ^{111}In-DOTA-GSG-J18 and varying concentrations of In-DOTA-GSG-J18 (10^{-13} to 10^{-4} M) for 1 h at 37°C. Cell-bound radioactivity was measured, and the IC_{50}-value was calculated using graphPad prism software.

Biodistribution of peptide ^{111}In-DOTA-GSG-J18 in SKOV-3 tumor-bearing nude mice

Nude mice (n=4) received tail-vein injections of approximately 0.17 Mbq of ^{111}In-GSG-DOTA-J18, and were subsequently housed separately. The animals were sacrificed by cervical dislocation at 30 min, 1 h, 2 h and 4 h post-injection, and organs were removed, weighed and counts were determined. Radioactive uptake in the tumor and in normal organs was calculated and expressed as percentage of injected dose per gram of tissue (%ID/g). For blocking experiments, tumor-bearing mice (n=4) were pre-injected with 100 μg nonradioactive In-DOTA-GSG-J18 peptide. After 5 min, the mice were injected with 0.17 MBq of ^{111}In-DOTA-GSG-J18, and the animals were sacrificed after 1 h and the blocking efficiency was evaluated.

Small animal SPECT/CT studies

Nude mice bearing xenografted SKOV-3 tumors were injected through the tail-vein with 13.0 MBq of ^{111}In-DOTA-GSG-J18 and imaged 1 h post-injection using a small-animal MicroCAT II SPECT/CT scanner (Siemens Medical Solutions, Malvern, PA) with a high-resolution 2 mm pinhole collimator at the Harry S. Truman Veterans Memorial Hospital Biomolecular Imaging Center. For blocking experiments, mice were pre-injected with 170 μg of nonradioactive In-labeled DOTA-GSG-J18 peptide. After 5 min, mice were injected with 13.0 MBq of ^{111}In-DOTA-GSG-J18 and imaged after a total of 1 h using a SPECT/CT scanner as described above.

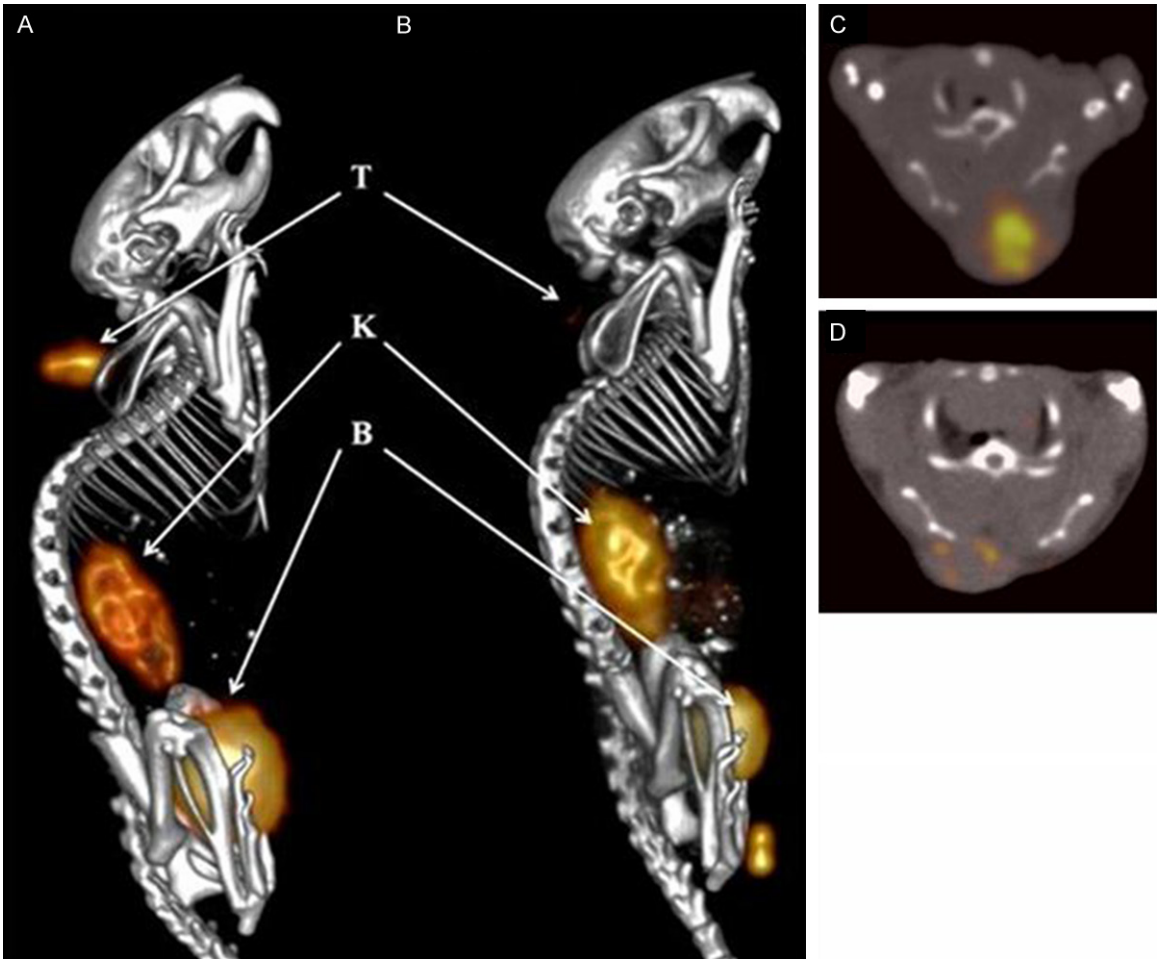

Figure 4. SPECT/CT study with nude mice carrying xenografted SKOV-3 tumors. (A) ^{111}In-DOTA-GSG-J18 (13.0 MBq) or (B) In-DOTA-GSG-J18 followed by ^{111}In-DOTA-GSG-J18 (13.0 MBq) were injected into the tail vein of SKOV-3 tumor-bearing nude mice. (C, D) Axial SPECT/CT images of tumor uptake of (C) ^{111}In-DOTA-GSG-J18 and (D) In-DOTA-GSG-J18 followed by ^{111}In-DOTA-GSG-J18. The live image was acquired 1 h post-injection under isoflurane anesthesia in a Siemens small-animal SPECT/CT scanner. The pictures show left lateral fused SPECT/CT images. T=tumor, K=kidneys and B=bladder. Created by 3D OSEM Fan beam (Feldkamp). Image processing was performed with Inveon Research Workplace processing software.

Statistical analysis

For statistical analysis an unpaired Student's t-test was performed to determine significance using Prism Graphpad Software. A *P*-value of 0.05 or less was considered significant.

Results

Phage display selection

In order to select peptides with good *in vivo* pharmacokinetic and tumor targeting properties, a two-tier phage display selection protocol was performed. In the last round of selection, 31 individual phage clones were identified, and were used in micropanning experiments to identify clones with high SKOV-3-to-HS-832 binding ratios. Results showed that phage clones pJ18 exhibited the highest SKOV-3-to-HS832 binding ratios of 6.57, indicating preferable binding to the human OC cell line (**Table 1**). Based on these results pJ18 was chosen for further analysis.

Peptide synthesis, radiolabeling and stability

Peptide J18 was synthesized with a GSG-spacer between the DOTA-group and the NH_2-terminus to avoid potential steric hindrance. The peptide (DOTA-GSG-J18) was successfully labeled with ^{111}In or non-radioactive In and purified by RP-HPLC. The radiolabeled peptide and its non-radioactive counterpart eluted with retention

times of 24.6 min and 24.5 min, respectively. High labeling efficiency of 98% and radiochemical purity of 98.6 ± 1.6% (mean ± SD), for ^{111}In-DOTA-GSG-J18 were observed. The yield of radiolabeled peptide was ~20% after HPLC and C-18 cartridge purification.

The stability of ^{111}In-DOTA-GSG-J18 was evaluated in mouse serum at 37°C for different time intervals and analyzed by RP-HPLC. Results showed that the radiolabeled peptide exhibited a half-life of 5.2 ± 0.43 h (mean ± SD) in mouse serum (**Figure 1**).

Cell binding

The specificity of ^{111}In-DOTA-GSG-J18 for OC cells was determined in a cell-binding assay using SKOV-3 and HS-832 cells. For this, ^{111}In-DOTA-GSG-J18 was incubated with 1x10^6 cells for different periods of time, and the bound radioactivity was measured and calculated as percentage of total counts per minute (% total cpm). Binding of the radiolabeled peptide to both cell lines increased from 0 min to 1 h, after which the binding gradually decreased. Nevertheless, in comparison to HS-832 cells, ^{111}In-DOTA-GSG-J18 exhibited significantly higher binding to SKOV-3 cells after 2 h, demonstrating specificity for this cell line (**Figure 2**).

Further validation of specific binding of radiolabeled peptide to SKOV-3 cells was determined by a competition assay in the presence of different concentrations of the correlating non-radioactive peptide. Results showed that the amount of bound radioactivity decreased in a dose-dependent manner with increasing concentrations of non-radiolabeled peptide, indicating that binding of ^{111}In-DOTA-GSG-J18 was out-competed by In-DOTA-GSG-J18 (**Figure 3**). Based on these data, an IC_{50} value of 10.5 ± 1.1 μM (mean ± SE) for ^{111}In-DOTA-GSG-J18 for SKOV-3 cells was calculated.

Pharmacokinetics of ^{111}In-GSG-DOTA-J18 peptide in SKOV-3 tumor-bearing nude mice

Indium-111 labeled DOTA-GSG-J18 peptide was evaluated in regard to its pharmacokinetic properties in nude mice bearing xenografted SKOV-3 tumors. Radioactive uptake in the tumor was calculated to be 1.63 ± 0.68, 0.60 ± 0.32, 0.31 ± 0.12 and 0.10 ± 0.02% ID/g at 30 min, 1 h, 2 h and 4 h, respectively (**Table 2**). The radioligand cleared from the blood and exhibited levels of 2.37 ± 0.94, 0.40 ± 0.24, 0.03 ± 0.03 and 0.19 ± 0.02% ID/g at 30 min, 1 h, 2 h and 4 h, respectively. The tumor-to-blood ratio increased from 0.69 at 30 min to 1.50 and 6.00 at 1 h and 2 h, respectively, indicating rapid blood clearance and kinetically favorable tumor uptake and retention. Equally high tumor-to-muscle ratios were observed as early as 1 h post-injection. Radioactive uptake in normal organs was, as expected, the highest in the kidneys due to renal clearance being the major route of excretion for most peptide ligands [16]. The kidney uptake was highest after 30 min at 6.71 ± 3.08 and decreased to 2.70 ± 0.95, 1.67 ± 0.43 and 1.75 ± 0.17% ID/g at 1 h, 2h and 4 h, respectively. Of all other organs, only the lungs, liver and spleen demonstrated noticeable radioligand uptake, which decreased rapidly after 1 h. Very little radioactivity was detected in the remaining organs and bone. In order to determine the specificity of tumor uptake, the radiolabeled peptide was subjected to an *in vivo* competition study with its non-radioactive counterpart. The results indicated that the non-radioactive peptide significantly blocked uptake of the radioactive counterpart by approximately 48%. The non-radioactive ligand did not significantly affect the uptake of ^{111}In-labeled peptide in normal organs.

SPECT/CT tumor imaging

The SPECT/CT imaging ability of ^{111}In-DOTA-GSG-J18 was evaluated in SKOV-3 xenografted nude mice (**Figure 4A**). The tumors were clearly visualized with high tumor-to background contrast, and the kidney uptake was concurrent with the pharmacokinetic data. Excretion of the radioligand was visible in the bladder, while little to no radioligand uptake was detected in other normal organs. Peptide tumor specificity was determined by blocking ^{111}In-DOTA-GSG-J18 tumor uptake in the presence of non-radioactive peptide. The image showed that radioactive tumor uptake was successfully blocked (**Figure 4B**), while radioactive uptake in the kidneys and other organs was unchanged, indicating that the radioligand exhibits specificity for SKOV-3 tumors.

Discussion

The poor prognosis of OC is a direct result of asymptomatic disease development and a lack

of adequate diagnostic techniques [1]. Many OC detection methods are under investigation; however, most show high specificity while exhibiting low sensitivity or *vice versa* [17, 18]. The need for new diagnostic tools combined with the fatality of OC, emphasizes the great need for development of efficacious detection methods.

Peptide-based radionuclide imaging agents are rapidly evolving due to implementation of combinatorial strategies including phage display technology [8, 9, 19]. While several peptides have been identified by *in vitro* phage display selections [20, 21], it is generally accepted that *in vivo* selections offer advantages in obtaining optimal targeting and pharmacokinetic properties [11, 12, 22-24]. A limited group of peptides have been identified in this manner, of which the most well-known example is identification of a RGD-containing peptide that binds vasculature expressed $\alpha_v\beta_3$-integrin, and has been employed in both positron emission tomography (PET) and SPECT imaging of the human tumor vasculature [22, 25, 26]. Other examples of peptides selected via *in vivo* phage display include the rhabdomyosarcoma targeting sequence CQQSNRGDRKRC [23], and several peptides that bind tumor vasculature receptors [11, 12, 24]. In contrast, our selection protocol initially selects for a sub-population of the library with desirable pharmacokinetics and extravasation abilities, which is followed by a subsequent *in vitro* selection that ensures tumor cell binding rather than vasculature targeting.

While many of these peptides show great promise; the majority of peptides target the tumor vasculature rather than tumor cells. Instead, our laboratory has developed a two-tier phage display screening method designed to select tumor-cell targeting peptides with high *in vivo* stability and good pharmacokinetic properties. The rigid screening process resulted in identification of peptide J18, which was synthesized with a DOTA-chelator and GSG-spacer and labeled with ^{111}In. The radiolabeled peptide demonstrated excellent stability under physiological conditions, indicating good potential *in vivo* stability [27]. A comparison of the binding patterns of the radiolabeled peptide for OC and normal ovarian cells were investigated, and although ^{111}In-DOTA-GSG-J18 showed minimal binding to HS-832 cells, the peptide exhibited significantly higher binding to SKOV-3 cells after 2 h. These results may indicate that the radiolabeled peptide binds to an antigen that is overexpressed by SKOV-3 cells, but is present at low levels on normal ovarian cells. Several cell receptors are known to exhibit such expression patterns, including the folate receptor-α and the ErbB2/Her2/neu receptor, among others [28, 29]. Competition studies demonstrated that binding of ^{111}In-DOTA-GSG-J18 to OC cells was specific, in that it was outcompeted by increasing concentrations of the correlating non-radioactive peptide. Based on this data, an IC_{50}-value of 10.5 ± 1.1 μM (mean ± SE) for the radiolabeled peptide was calculated, which is in correlation with what has previously been reported for phage display peptides selected against live cells [30].

A competition biodistribution study with ^{111}In-DOTA-GSG-J18 in the presence of non-radiolabeled peptide demonstrated specific binding to the tumor, while radioactive uptake in other organs was non-specific. Additionally, low levels of radioactivity in the blood as well as rapid clearance indicated good stability of the radionuclide-chelator complex as free ^{111}In would bind to metal conjugating serum proteins resulting in prolonged circulation. Both the small molecular size and the positive charge of the peptide at physiological pH indicate that the majority should be cleared through the kidneys. This is evident from the biodistribution results, and correlates with the fact that renal clearance is the preferred route of excretion for most radiolabeled peptides [16]. Renal retention of radiolabeled compounds may lead to nephrotoxicity [31]. However, kidney uptake of ^{111}In-DOTA-GSG-J18 rapidly decreased after only 1 h, thereby minimizing potential kidney exposure. Low non-specific retention of radioactivity in the liver and spleen may be due to hydrophobicity of the peptide and the fact that increased lipophilicity tends to direct a compound towards hepatic excretion [32]. Finally, the lungs showed some non-specific retention of radioactivity, which may be due to high perfusion and increased exposure to the blood circulation.

In vivo SPECT/CT imaging of SKOV-3 xenografted mice using ^{111}In-DOTA-GSG-J18 revealed high tumor-to-background ratios, and successfully localized the tumor. In correlation with the pharmacokinetic studies, the majority of the radioactivity was found in the kidneys, and

renal excretion of the peptide was clearly evident from high levels in the bladder. Furthermore, tumor uptake of the radioactive peptide was successfully blocked by injection of the non-radioactive counterpart showing specificity of the peptide for the SKOV-3 tumor.

To date, very few *in vivo* OC imaging agents have been reported. Of the few, a tetrameric vascular cell adhesion molecule 1 (VCAM-1) targeting peptide is among the most successful. Although the VCAM-1 targeting peptide exhibited excellent tumor homing, its use is limited to advanced stages of OC. In fact, VCAM-1 was not detectable on stage I tumors [9]. The peptide 18-DOTA was employed in successful SPECT/CT imaging of SKOV-3 metastases in mice and showed prolonged tumor retention and minimal radioactive uptake in normal organs. In order to further improve binding affinity, tumor uptake and retention, affinity maturation, alanine scanning, or display of the peptide as multiple copies on a scaffold may be performed in future studies. Additionally, identification of the peptide antigen will aid in the optimization of the targeting agent, and potentially shed light upon the pathology of ovarian cancer. Currently, the antigen remains unknown; however, future studies including proteomic analysis will be performed.

Here, we demonstrated that ^{111}In-DOTA-GSG-J18 images xenografted human ovarian SKOV-3 tumors in live nude mice using SPECT/CT, and exhibits rapid renal clearance. This peptide may be useful in advancing the diagnosis of OC and allows detection of early stages of the malignancy.

Conclusion

The SKOV-3 specific peptide J18 was selected by a two-tier phage display screening process and evaluated for its binding, pharmacokinetic and SPECT/CT imaging properties. The peptide demonstrated good tumor uptake and retention and successfully imaged SKOV-3 tumors in xenografted nude mice. In conclusion, the J18 peptide may be an effective imaging agent of OC.

Acknowledgements

We acknowledge the contributions of Lisa Watkinson, Terry Carmack and Marie Dickerson. This work was supported by a Veterans Affairs (VA) Merit Review Award BX000964 and the National Institutes of Health (NIH) 1R21CA-134960.

Disclosure of conflict of interest

None.

Address correspondence to: Dr. Susan L Deutscher, Department of Biochemistry, University of Missouri, Rm117 Schweitzer Hall, Columbia, MO 65211, USA. Tel: 573-882-2454; Fax: 573-884-4597; E-mail: deutschers@missouri.edu

References

[1] Aletti GD, Gallenberg MM, Cliby WA, Jatoi A and Hartmann LC. Current Management Strategies for Ovarian Cancer. Mayo Clin Proc 2007; 82: 751-770.

[2] Siegel R, Naishadham D and Jemal A. Cancer statistics, 2013. CA Cancer J Clin 2013; 63: 11-30.

[3] Neesham D. Ovarian cancer screening. Aust Fam Physician 2007; 36: 126-128.

[4] Bakker WH, Krenning EP, Reubi JC, Breeman WA, Setyono-Han B, de Jong M, Kooij PP, Bruns C, van Hagen PM, Marbach P, et al. In vivo application of [111In-DTPA-D-Phe1]-octreotide for detection of somatostatin receptor-positive tumors in rats. Life Sci 1991; 49: 1593-1601.

[5] Chen J, Cheng Z, Miao Y, Jurisson SS and Quinn TP. Alpha-melanocyte-stimulating hormone peptide analogs labeled with technetium-99m and indium-111 for malignant melanoma targeting. Cancer 2002; 94: 1196-1201.

[6] Deutscher SL, Figueroa SD and Kumar SR. In-labeled KCCYSL peptide as an imaging probe for ErbB-2-expressing ovarian carcinomas. J Labelled Comp Radiopharm 2009; 52: 583-590.

[7] Behr TM, Gotthardt M, Barth A and Behe M. Imaging tumors with peptide-based radioligands. Q J Nucl Med 2001; 45: 189-200.

[8] Karasseva NG, Glinsky VV, Chen NX, Komatireddy R and Quinn TP. Identification and characterization of peptides that bind human ErbB-2 selected from a bacteriophage display library. J Protein Chem 2002; 21: 287-296.

[9] Scalici JM, Thomas S, Harrer C, Raines TA, Curran J, Atkins KA, Conaway MR, Duska L, Kelly KA and Slack-Davis JK. Imaging VCAM-1 as an Indicator of Treatment Efficacy in Metastatic Ovarian Cancer. J Nucl Med 2013; 54: 1-7.

[10] Smith GP. Filamentous fusion phage: novel expression vectors that display cloned antigens

on the virion surface. Science 1985; 228: 1315-1317.
[11] Arap W, Kolonin MG, Trepel M, Lahdenranta J, Cardo-Vila M, Giordano RJ, Mintz PJ, Ardelt PU, Yao VJ, Vidal CI, Chen L, Flamm A, Valtanen H, Weavind LM, Hicks ME, Pollock RE, Botz GH, Bucana CD, Koivunen E, Cahill D, Troncoso P, Baggerly KA, Pentz RD, Do KA, Logothetis CJ and Pasqualini R. Steps toward mapping the human vasculature by phage display. Nat Med 2002; 8: 121-127.
[12] Yao VJ, Ozawa MG, Trepel M, Arap W, McDonald DM and Pasqualini R. Targeting pancreatic islets with phage display assisted by laser pressure catapult microdissection. Am J Pathol 2005; 166: 625-636.
[13] Newton JR, Kelly KA, Mahmood U, Weissleder R and Deutscher SL. In vivo selection of phage for the optical imaging of PC-3 human prostate carcinoma in mice. Neoplasia 2006; 8: 772-780.
[14] Clarke C, Titley J, Davies S and O'Hare MJ. An immunomagnetic separation method using superparamagnetic (MACS) beads for large-scale purification of human mammary luminal and myoepithelial cells. Epithelial Cell Biol 1994; 3: 38-46.
[15] Kumar SR and Deutscher SL. 111In-labeled galectin-3-targeting peptide as a SPECT agent for imaging breast tumors. J Nucl Med 2008; 49: 796-803.
[16] Vegt E, de Jong M, Wetzels JFM, Masereeuw R, Melis M, Oyen WJG, Gotthardt M and Boerman OC. Renal Toxicity of Radiolabeled Peptides and Antibody Fragments: Mechanisms, Impact on Radionuclide Therapy, and Strategies for Prevention. J Nucl Med 2010; 51: 1049-1058.
[17] Leung F, Diamandis EP and Kulasingam V. From bench to bedside: discovery of ovarian cancer biomarkers using high-throughput technologies in the past decade. Biomark Med 2012; 6: 613-625.
[18] Su Z, Graybill WS and Zhu Y. Detection and monitoring of ovarian cancer. Clin Chim Acta 2013; 415: 341-345.
[19] Peletskaya EN, Glinsky G, Deutscher SL and Quinn TP. Identification of peptide sequences that bind the Thomsen-Friedenreich cancer-associated glycoantigen from bacteriophage peptide display libraries. Molec Divers 1996; 2: 13-18.
[20] Leinonen J, Wu P, Koivunen E, Narvanen A and Stenman UH. Development of novel peptide ligands modulating the enzyme activity of prostate-specific antigen. Scand J Clin Lab Invest Suppl 2000; 233: 59-64.
[21] Koistinen H, Narvanen A, Pakkala M, Hekim C, Mattsson JM, Zhu L, Laakkonen P and Stenman UH. Development of peptides specifically modulating the activity of KLK2 and KLK3. Biol Chem 2008; 389: 633-642.
[22] Pasqualini R and Ruoslahti E. Organ targeting in vivo using phage display peptide libraries. Nature 1996; 380: 364-366.
[23] Witt H, Hajdin K, Iljin K, Greiner O, Niggli FK, Schafer BW and Bernasconi M. Identification of a rhabdomyosarcoma targeting peptide by phage display with sequence similarities to the tumour lymphatic-homing peptide LyP-1. Int J Cancer 2009; 124: 2026-2032.
[24] Essler M and Ruoslahti E. Molecular specialization of breast vasculature: a breast-homing phage-displayed peptide binds to aminopeptidase P in breast vasculature. Proc Natl Acad Sci 2002; 99: 2252-2257.
[25] Chen X, Park R, Tohme M, Shahinian AH, Bading JR and Conti PS. MicroPET and autoradiographic imaging of breast cancer alpha v-integrin expression using 18F- and 64Cu-labeled RGD peptide. Bioconjug Chem 2004; 15: 41-49.
[26] Liu S, Hsieh WY, Jiang Y, Kim YS, Sreerama SG, Chen X, Jia B and Wang F. Evaluation of a (99m)Tc-labeled cyclic RGD tetramer for noninvasive imaging integrin alpha(v)beta3-positive breast cancer. Bioconjug Chem 2007; 18: 438-446.
[27] Jain RK. Delivery of molecular and cellular medicine to solid tumors. J Control Release 1998; 53: 49-67.
[28] Ross JF, Chaudhuri PK and Ratnam M. Differential regulation of folate receptor isoforms in normal and malignant tissues in vivo and in established cell lines. Physiologic and clinical implications. Cancer 1994; 73: 2432-2443.
[29] Hung MC, Zhang X, Yan DH, Zhang HZ, He GP, Zhang TQ and Shi DR. Aberrant expression of the c-erbB-2/neu protooncogene in ovarian cancer. Cancer Lett 1992; 61: 95-103.
[30] Ma C, Yin G, Yan D, He X, Zhang L, Wei Y and Huang Z. A novel peptide specifically targeting ovarian cancer identified by in vivo phage display. J Pept Sci 2013; 19: 730-736.
[31] Wessels BW, Konijnenberg MW, Dale RG, Breitz HB, Cremonesi M, Meredith RF, Green AJ, Bouchet LG, Brill AB, Bolch WE, Sgouros G and Thomas SR. MIRD pamphlet No. 20: the effect of model assumptions on kidney dosimetry and response--implications for radionuclide therapy. J Nucl Med 2008; 49: 1884-1899.
[32] Hosseinimehr SJ, Tolmachev V and Orlova A. Liver uptake of radiolabeled targeting proteins and peptides: considerations for targeting peptide conjugate design. Drug Discov Today 2012; 17: 1224-1232.